SciMedCentral

JSM Nanotechnology & Nanomedicine

Research Article

A Detailed First Principles Investigation of Optical Properties of Monolayer T-Graphene Sheet and Nanoribbon

Arka Bandyopadhyay and Debnarayan Jana*

Department of Physics, University of Calcutta, India

***Corresponding author**

Debnarayan Jana, Department of Physics, University of Calcutta, 92 A.P.C Road, Kolkata-700009, India, Email: djphy@caluniv.ac.in

Submitted: 24 October 2017

Accepted: 11 November 2017

Published: 16 November 2017

ISSN: 2334-1815

Keywords

- Density functional theory; Tetragonal graphene; Nanoribbon; Optical properties

Abstract

In this first principles investigation, we have analysed the refractive indices, optical absorption and conductivity spectra of tetragonal graphene sheet and its experimentally realized substructure, the narrowest arm chair nanoribbon. It is noteworthy that, the oscillatory behaviours encountered in the optical responses are shifted towards the UV region under perpendicular polarization. The real part of refractive index spectra exhibit anisotropic nature for both the systems. This anisotropy leads to the anomalous dispersion near certain frequencies where attenuation peaks are also observed. A particular example is that, the violet light of energy 2.94 eV undergoes maximum attenuation when parallel polarized EM wave propagates through the sheet. Besides, the maximum peak position of absorption and attenuation spectra coincides for perpendicularly polarized light. In addition, the conductivity and absorption spectra show identical behaviour under a particular type of polarization. Our observations strongly support the fact that, these optically active, non-hexagonal, anisotropic materials can be used as birefringent in future nano-electronic devices.

INTRODUCTION

First experimental isolation of single-layer graphene [1], sheet from graphite has amazed the world of science in the last decade. Its spectacular mechanical, electrical, thermodynamic and optical properties have motivated researchers in both scientific and industrial research [2,3]. In particular, the ultrahigh carrier mobility [4], fractional, fractal and half-integer Hall effects [5-11], have secured its coronation as a revolutionary material of the post-silicon era [12]. Despite all the intriguing features, the only dispute that restricts the industrial revolution of making graphene based nano devices is its zero band gap. However, several attempts have been made to overcome this drawback [13-19]. As a historical note, the story of graphene was initiated by German mathematician Johannes Kepler [20], in the seventeenth century. He proposed only 13 different possibilities that a structure can be constructed from regular polygons and identical vertices to which these polygons adjoin [21]. Hexagonal structure graphene is a crystalline form of one of those possibilities. Furthermore, Balaban [22] proposed the theoretical existence of other two dimensional (2D) carbon materials with different complex hybridizations. In a recently study on different graphene allotropes, Enyashin et al. [23], have studied the stability and electronic properties of 12 such configurations. Graphyne [24], and graphdiyne [25], are two particular examples of such graphene allotropes that were experimentally realized [26-29]. Another member of the family of Kepler nets [20], comprises both squares and octagons have also motivated the researchers [23,30, 31]. Liu et al. [32], have recently named the structure as tetragonal graphene or T graphene (TG) and have unravel its structural and electronic properties in the framework of density functional theory (DFT) study. The planar TG sheet exhibits metallic nature and is thermodynamically more stable than any other graphene allotropes including experimentally achieved graphyne and graphdiyne. Another buckled form of TG was predicted [32], to be stable in the high temperature, but subsequently opposed by Kim et al., [33]. Moreover, Kotakoski et al. [34] have experimentally obtained a small part of the narrowest armchair planar TG nanoribbon (NATGNR) with the help of electron beam irradiation on graphene. Motivated by all these, Ye et al. [35], have decorated the TG sheet with Li atoms to explore that it can serve as a good reversible hydrogen storage material. Liu et al. [36], further added that Li decorated TG exhibits a high sensitivity to carbon monoxide (CO). Therefore, it can be used in CO sensor devices. Besides, TG analogous tetragonal carbon-boron-nitrogen (CBN) and boron-nitrogen (BN) sheets exhibit semiconducting nature [37], which is essential for device applications. The characterizing Raman fingerprints of TG sheet has been explored [38], using variable cluster approach [39]. Furthermore, Chowdhury et al. [40], have investigated the effect of transition metal atoms doping on TG and explored that Mn doped system possess highest magnetic moments. In addition, they have also observed that the magnitude of the magnetic moment increases with increasing atomic weight. It is worthy to note that,

the same structure has also been investigated as octagraphene [41,42], and planar c_4 sheet [43]. The metallic nature of TG sheet also restricts its possibilities in device application. Therefore, Bandyopadhyay et al. [44], have switched on external localized magnetic fluxes and tuned the band gap with different choices of magnetic fluxes linked with two different rings of TG sheet and the NATGNR [34]. Additionally, the width dependent electronic transport properties of TGNRs have been calculated by Dai et al. [45]. Similar to the TG structure, there exist many other 2D materials [46-50], with the possibility of different structure dependent opto electronic properties.

In our previous work [44], we have critically evaluated some of the optical properties of the TG sheet and the NATGNR in the secure of DFT. However, the complete description of optical responses are yet to be reported. Here, our primary aim is to address the frequency dependent complex refractive index, optical absorption spectra and optical conductivity in the long wavelength limit. This paper is organized as follows. In the next section, the methodology adapted for this study is explained, followed by different results related to the optical behaviour of the TG sheet and the NATGNR and finally conclusions are drawn at the end.

COMPUTATIONAL METHODOLOGY

In this work, we have extensively used density functional theory (DFT) with generalized gradient approximation (GGA) as implemented in SIESTA package [51-53]. The Perdew-Burke-Ernzerhof (PBE) is used for the exchange-correlation part of density functional. The real space mesh cutoff is chosen to be 300 Ry throughout the calculation. The Brillouin zone sampling is performed with 21×21×1 and 21×1×1 Monkhorst-Pack (MP) set of k points [54], for sheet and the NRs respectively. A vacuum slab of 20$\AA$ is used to avoid any interaction between layers. Total energy cut off for the self-consistent field (SCF) is fixed at 10^{-5} eV at an electronic temperature 300 K. The most stable configuration is achieved by a structural relaxation with convergence criteria for maximum force on each atom below 0.001 eV/$\AA$. Optical properties are calculated for real interband transitions ie., transition between occupied and unoccupied states in terms of frequency (ω, in energy unit) dependent dielectric function $\varepsilon(\omega) = \varepsilon_1(\omega) + i\varepsilon_2(\omega)$. At first, the imaginary part $\varepsilon_2(\omega)$ is estimated using first order time dependent perturbation theory in the dipole approximation in the long wavelength limit (q---->0) [55-57] given by

$$\in_2(\omega) = \frac{2\pi e^2}{\Omega\varepsilon_0} \sum_{k,VB,CB} \left| \langle \varphi_K^{VB} \left| \vec{u}.\vec{r} \right| \varphi_K^{CB} \rangle \right|^2 \delta(E_K^{CB} - E_K^{VB} - \omega). \quad (1)$$

Where, Ω, ε_0, $\vec{u}$, $\vec{r}$ represent volume of the supercell, free space dielectric constant, polarization vector of electric field and position vector respectively. In this calculation, reasonably large number of empty bands (*NBANDs* =400), have been included to avoid inconsistency in the dielectric spectra [58]. Furthermore, the real part $\varepsilon_1(\omega)$ has been calculated from the imaginary part with the help of Kramers-Kronig (KK) relation. Other optical properties, ie., real ($n(\omega)$), imaginary ($k(\omega)$) part of complex refractive index ($N(\omega)$), optical absorption ($\alpha(\omega)$) and optical conductivity ($\sigma(\omega)$) are calculated from $\varepsilon_1(\omega)$ and $\varepsilon_2(\omega)$. The relations can be expressed as follows.

$$N(\omega) = n(\omega) + ik(\omega) = \sqrt{\varepsilon(\omega)} \quad (2)$$

$$n(\omega) = \left(\frac{\sqrt{\varepsilon_1^2 + \varepsilon_2^2} + \varepsilon_1}{2} \right)^{\frac{1}{2}} \quad (3)$$

$$k(\omega) = \left(\frac{\sqrt{\varepsilon_1^2 + \varepsilon_2^2} - \varepsilon_1}{2} \right)^{\frac{1}{2}} \quad (4)$$

$$\alpha(\omega) = \frac{2\omega k(\omega)}{c\hbar} \quad (5)$$

$$\sigma(\omega) = \frac{\omega\varepsilon_2(\omega)}{4\pi} \quad (6)$$

In the above expressions c represents the speed of light in vacuum. Here it is worthy to mention that, the excitonic effects will give no other effect than enhancing the peak values. Therefore, excitonic effects are not taken into account during the calculations. All the results obtained from the above equations are describes in specific sections. In parallel (perpendicular) polarization, the electric field is applied along an axis parallel (perpendicular) to the plane of the sheet.

RESULTS AND DISCUSSION

The optimized structure of TG sheet consists of two distinct bond lengths 1.47 Å (d_1) and 1.38 Å (d_2), as shown in Figure 1. The NATGNR, indicated within the red box in Figure 1 can be achieved after cutting the sheet along the x-y direction. As mentioned earlier, the detailed descriptions on the structural, electronic and some of the optical properties ie., frequency dependent dielectric function, reflectivity and electron energy loss spectra are already reported in our earlier work [44]. Therefore in this

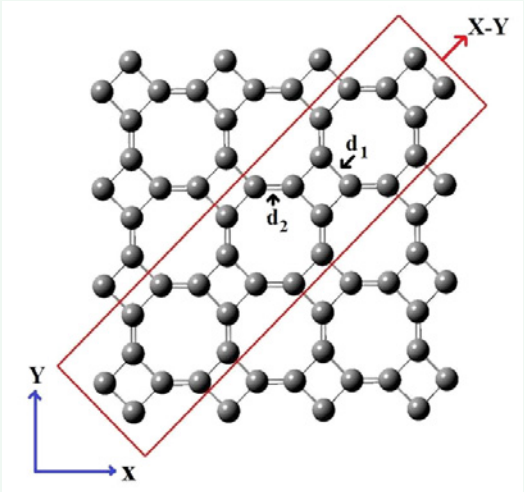

Figure 1 Structure of TG sheet. d_1 and d_2 are two distinct bond lengths. The NATGNR is indicated within red box.

section, we have critically analysed the complex refractive index, optical absorption and conductivity spectra of the sheet and the NATGNR to get complete description of their optical behavior. All the optical responses are calculated for photon energies upto 30 eV which, gives the relevant information in the ultraviolet (UV), visible (VIS) and infrared limits (IR) of the electromagnetic spectra. Results are described in the specific subsections.

Refractive index

The real ($n(\omega)$) and imaginary ($k(\omega)$) parts of the refractive index have been calculated with the help of Eq.3 and Eq.4. Here, $n(\omega)$ accounts the refraction, while, $k(\omega)$ governs the attenuation of EM wave passes through the material. The $k(\omega)$ is known as the extinction coefficient. These two parameters are related by Kramers–Kronig relations.

In the TG sheet, the $n(\omega)$ at very low energy (0.06 eV, from here interband transition contribute significantly) have the values 1.31 and 1.08 for parallel and normal incidences respectively. It is worthy to note that, these values are invariably smaller compared to the static refractive indices of graphene ($n_{\parallel}(0)$=2.75 and $n_{\perp}(0)$=1.12) [59]. The spectral pattern of $n(\omega)$ (depicted in Figure 2) is fluctuating in nature which results several intense peaks in the $k(\omega)$ spectra. This result is a direct consequence of the Kramers–Kronig relation between these two parameters. If we expose TG sheet under parallel incidence, $k(\omega)$ exhibits the highest peak for the violet light (at 2.94 eV) of the visible region. This peak can be well explained from the anomalous behaviour of dispersion curve ($n(\omega)$) near the mentioned frequency. In the vicinity of the above discussed energy, there is another anomalous dispersion region near 3.56 eV, which results another $k(\omega)$ peak in the near ultraviolet region. Above this frequency, there is a zone of normal dispersion in the frequency interval 5.28 - 9.92 eV. This indicates practically negligible loss of energy of EM wave within this frequency range while passing through the sheet. There are some other attenuation peaks in parallel incidence. Some of them are as follows.

Parallel incidence: 2.94 eV (maximum), 3.56 eV, 4.54 eV, 10.14 eV, 11.52 eV, 12.24 eV, 12.98 eV, 13.74 eV, 14.35 eV, 14.98 eV, 15.64 eV, 16.84 eV, 18.78 eV, 22.24 eV. Besides, for the normal incidence, we have obtained relatively low intense peaks in the $k(\omega)$ spectra. This is due to the relatively smooth nature of $n(\omega)$ under normal incidence compared to the parallel incidence. In this case, $n(\omega)$ shows essentially no variation till 10 eV. Therefore, all the visible lights and near ultraviolet lights will pass through without any attenuation under normal incidence. In the higher energy regions however, some attenuation peaks occur which is again supported by the anaisotropic nature of $n(\omega)$ in this region. Some of the appreciable attenuation peaks are listed as follows.

Normal incidence: 13.06 eV, 13.99 eV, 14.73 eV, 17.28 eV, 18.12 eV, 18.76 eV, 19.96 eV (maximum), 20.86 eV, 21.98 eV, 22.54 eV, 25.40 eV, 26.64 eV, 27.24 eV etc.

Similarly for the NATGNR, $n(\omega)$ fluctuates more rapidly in the low energy (higher energy) regions when exposed to

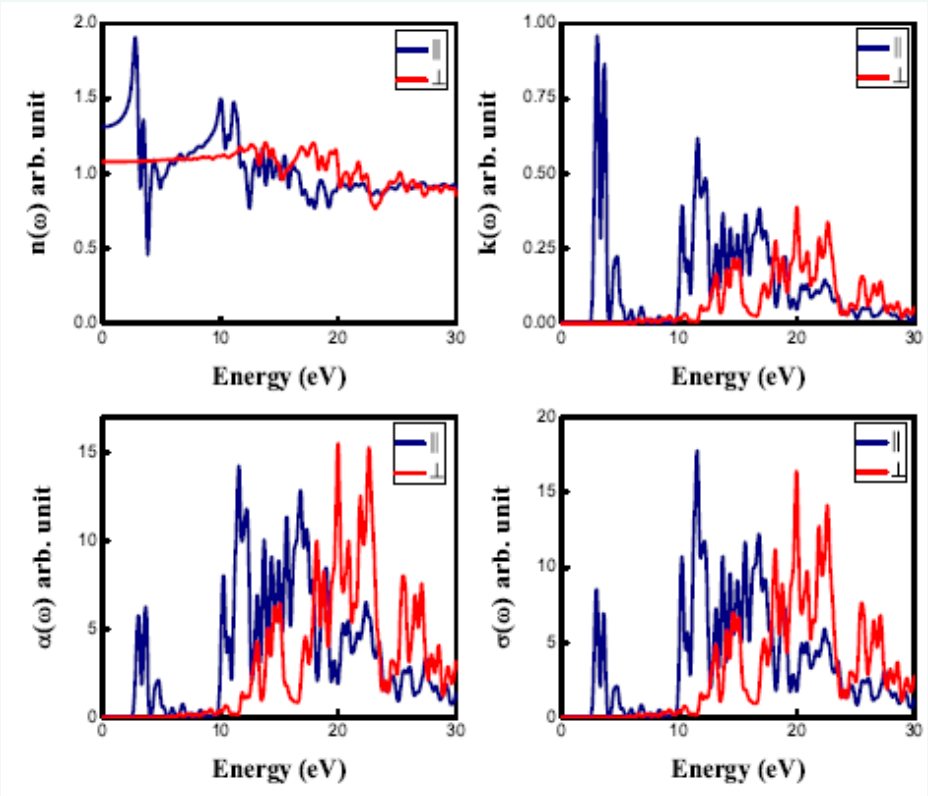

Figure 2 Real ($n(\omega)$) and imaginary ($k(\omega)$) parts of refractive index, absorption coefficient ($\alpha(\omega)$) and conductivity spectra ($\sigma(\omega)$) of TG sheet. Blue and red lines indicate parallel and perpendicular polarization.

parallel (perpendicular) incidence as depicted in Figure 3. These fluctuations give rise to various $k(\omega)$ peaks as mentioned earlier. The $n(\omega)$ at very low energy (0.06 eV, from here interband transition contribute significantly) have the values 1.15 and 1.02 for parallel and perpendicular polarizations respectively. The $n(\omega)$ shows attenuation peaks near the following values.

Parallel incidence: 0.5 eV, 1.84 eV, 2.7 eV, 3.46 eV, 4.16 eV, 4.92 eV, 5.80 eV (maximum), 10.00 eV, 12.38 eV, 13.24 eV, 14.10 eV, 14.74 eV, 17.89 eV etc;

Normal incidence: 13.10 eV, 14.04 eV, 15.08 eV, 16.04 eV, 16.98 eV, 18.98 eV (maximum), 19.82 eV, 20.50 eV, 21.34 eV, 27.08 eV etc. Therefore it is clear that, parallel polarized light with energy ranging between 6.46 and 6.46 eV will experience no attenuation while passing through the NATGNR. Similarly, under normal incidence no attenuation occurs below the energy 10 eV.

Optical absorption

Absorption spectra ($\alpha(\omega)$) have been calculated from Eq.5. It is found that, the $\alpha(\omega)$ spectra is highly anisotropic in nature and its peak positions are in well agreement with the $\varepsilon_2(\omega)$ and $k(\omega)$ spectra. A detailed description of the $\varepsilon_2(\omega)$ spectra have been reported in our earlier work [44]. The absorption peaks correspond to different intraband transitions in the electronic band structures. Under parallel incidence, sheet does not absorb EM wave below energy 2.32 eV (Figure 2). Above that, three consecutive $\alpha(\omega)$ peaks have been observed at 3.00 eV, 3.60 eV and 4.60 eV. Further, no absorption region is found within 5.36 eV and 9.78 eV. Several intense peaks occur above 10 eV, a few are listed below.

Parallel incidence : 10.20 eV, 11.56 eV (maximum), 12.22 eV, 13.04 eV, 13.62 eV, 14.28 eV, 14.92 eV, 15.52 eV, 16.64 eV, 17.38 eV, 17.88 eV, 18.88 eV, 20.72 eV, 22.48 eV, 23.48 eV, 24.50 eV, 25.70 eV, 27.56 eV etc. Besides, there is literally no absorption of normally incident EM wave with energy below 10 eV on the sheet. TG sheet absorb lights with more energy under normal incidence. In this case the peaks are observed at the following energies.

Normal incidence: 13.08 eV, 14.14 eV, 14.54 eV, 17.13 eV, 18.20 eV, 18.76 eV, 20.02 eV (maximum), 20.86 eV, 21.82 eV, 22.50 eV, 24.72 eV, 25.46 eV, 26.44 eV, 27.08 eV, 28.62 eV etc.

Similar to the sheet, the absorption spectra of NATGNR also supports the attenuation spectra. Therefore, the energy intervals in which attenuation has zero value, absorption have also zero value. This supports the fact of unperturbed propagation of EM waves with those energies. The maximum peak positions of $k(\omega)$ and $\alpha(\omega)$ coincides for NATGNR under perpendicular polarization. However, the maximum peak of $\alpha(\omega)$ is blue shifted compared to that of the $k(\omega)$ peak under parallel polarization. In this case, the maximum value of $\alpha(\omega)$ is observed near 13.40 eV.

Optical conductivity

The optical conductivity spectra are calculated for both the systems with the help of Eq.6. These conductivity spectra closely follow the absorption

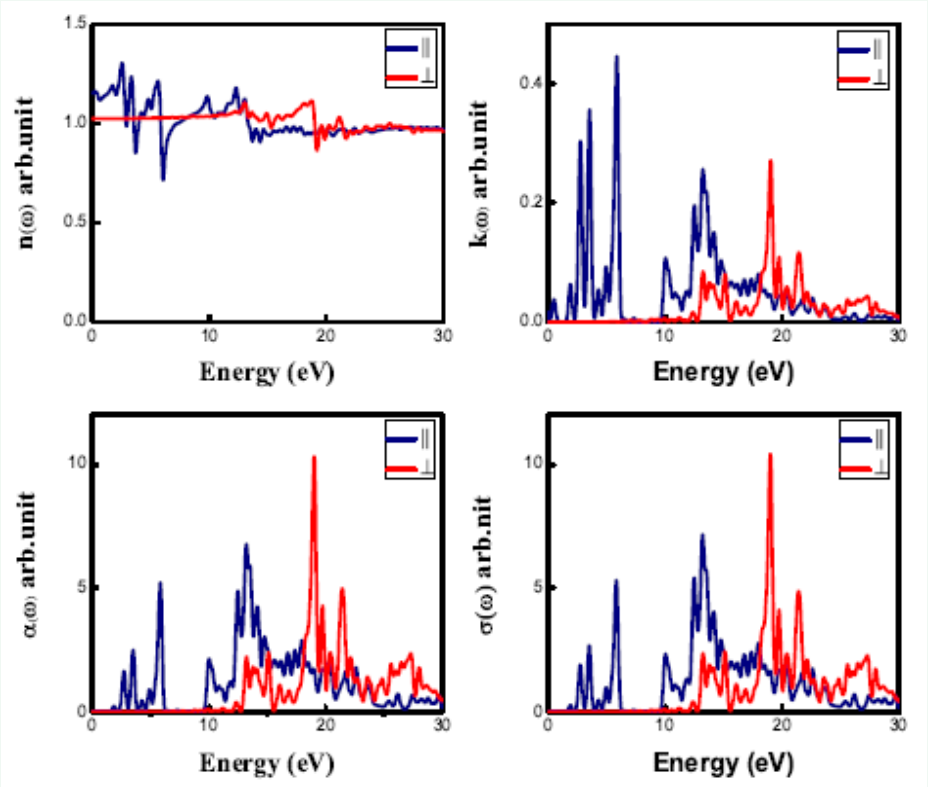

Figure 3 Real ($n(\omega)$) and imaginary ($k(\omega)$) parts of refractive index, absorption coefficient ($\alpha(\omega)$) and conductivity spectra ($\sigma(\omega)$) of NATGNR. Blue and red lines indicate parallel and perpendicular polarization.

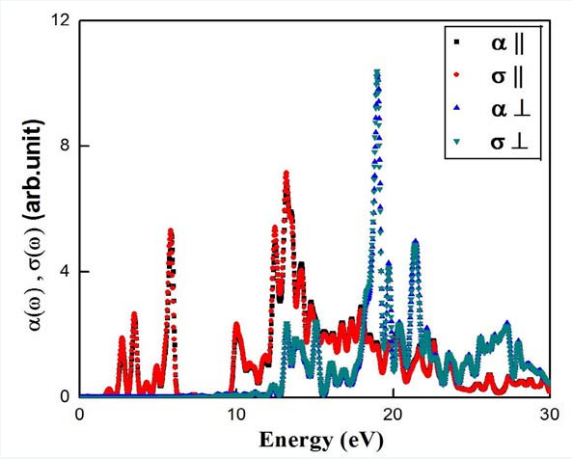

Figure 4 Optical conductivity and absorption spectra of NATGNR exhibit indistinguishable nature for parallel as well as perpendicular polarization.

Coefficient appreciably for both types of polarizations. The optical gaps determine the threshold above which considerable amount of conduction takes place. The gap is found to be 2.46 eV and 6.32 eV for the sheet under parallel and normal incidence respectively. Some prominent conductivity peak positions within our calculation limits are given as follows.

Parallel incidence: 2.82 eV, 3.58 eV, 4.58 eV, 10.14 eV, 11.38 eV (maximum), 12.98 eV, 13.62 eV, 14.22 eV, 14.96 eV, 15.48 eV, 16.58 eV, 17.12 eV, 18.82 eV, 20.38 eV, 22.30 eV, 23.54 eV, 24.54 eV, 25.54 eV, 27.46 eV, 29.16 eV etc;

Normal incidence: 11.72 eV, 13.04 eV, 14.08 eV, 14.48 eV, 14.96 eV, 17.20 eV, 18.08 eV, 18.70 eV, 19.96 eV (maximum), 20.80 eV, 21.90 eV, 22.46 eV, 25.54 eV, 26.62 eV, 27.16 eV, 28.50 eV etc.

It is noteworthy that, the $\sigma(\omega)$ spectra of the NATGNR is in well agreement with the $\alpha(\omega)$ spectra as shown in Figure 4. Therefore it is clear that, the electronic transitions which give rise to the maximum absorption of NATGNR also leads to maximum conduction. These results will shed light on possibilities of the device applications of the TG sheet and NATGNR.

CONCLUSION

In this work, we have critically analysed different optical properties of TG sheet and NATGNR calculated from first principles study. The following conclusions can be made from the above discussions. When the sheet is ex-posed under parallel polarization, the lower limiting value of the refractive index is observed to be 1.31 and the same for NATGNR is 1.15. However, for perpendicular polarization the same have the values 1.08 (sheet) and 1.02 (NATGNR). Therefore, sheet always possesses the larger value compared to NATGNR. Besides, the oscillatory behaviour of all the optical responses is shifted towards the higher energy region or UV region under perpendicular polarization. The $n(\omega)$ spectra of the sheet and ribbon are anisotropic in nature under both polarizations and exhibit anomalous dispersion in each of the cases. The sheet under parallel polarization shows isotropic behavior well above 20 eV and the same under perpendicular polarization happens below 10 eV. However, for the NATGNR, the isotropic behaviors are observed above 15 eV for parallel polarization and below 10 eV. In the later case $n(\omega)$ is less oscillatory in nature. Each anomalous dispersion corresponds to an attenuation peak in $k(\omega)$ spectra for all the cases. This is simply due to the Kramers–Kronig relation between them. The sheet exhibits maximum attenuation of violet light of energy 2.94 eV among other EM waves with different frequencies. All the results mentioned above strongly support the fact that these optically active anisotropic materials can be used as birefringent. Furthermore, absorption spectra almost mimic the attenuation spectra. However, relative peak intensities are modified significantly. The maximum peak position of $k(\omega)$ and $\alpha(\omega)$ spectra coincide for both the systems under perpendicularly polarized light. However, the maximum absorption peak is blue shifted compared to the attenuation peak under parallel polarization. In addition, $\sigma(\omega)$ and $\alpha(\omega)$ spectra of the NATGNR are almost indistinguishable under each type of polarizations. We expect, our results will enhance the possibilities of using TG and its nanoribbons in future optoelectronic nano devices.

ACKNOWLEDGEMENTS

This work is funded by the DST-FIST, DST-PURSE, Government of India. One of the authors (AB) sincerely acknowledges the University of Calcutta for university research fellowship.

REFERENCES

1. Novoselov KS, Geim AK, Morozov SV, Jiang D, Zhang Y, Dubonos SV, et al. Electric field effect in atomically thin carbon films. Science. 2004; 306: 666-669.
2. Castro Neto AH, Guinea F, Peres NMR, Novoselov KS, Geim AK. The electronic properties of graphene. Rev Mod Phys. 2009; 81: 109-162.
3. Geim AK. Graphene: status and prospects. Science. 2009; 324: 1530-1534.
4. Bolotin KI, Sikes KJ, Jiang Z, Kilma M, Fudenberg JH, Kim P, et al. Ultrahigh electron mobility in suspended graphene. Solid State Commun. 2008; 146: 351-355.
5. Novoselov KS, Geim AK, Morozov SV, Jiang D, Katsnelson MI, Grigorieva IV, et al. Two dimensional gas of massless Dirac fermions in graphene. Nature. 2005; 438: 197-200.
6. Zhang YB, Tan YW, Stormer H L, Philip Kim. Experimental observation of the quantum Hall effect and Berry's phase in graphene. Nature. 2005; 438: 201-204.
7. Bolotin K I, Ghahari F, Shulman MD, Horst L. Stormer, Philip Kim. Observation of the fractional quantum Hall effect in graphene. Nature. 2009; 462: 196-199.
8. Du X, Skachko I, Duerr F, Adina Luican, Eva Y. Andrei. Fractional quantum Hall effect and insulating phase of Dirac electrons in graphene. Nature. 2009; 462: 192-195.
9. Ponomarenko LA, Gorbachev RV, Yu GL, Elias DC, Jalil R, Patel AA, et al. Cloning of Dirac fermions in graphene superlattices. Nature. 2013; 497: 594-597.
10. Hunt B, Sanchez-Yagishi JD, Young AF, Yankowitz M, LeRoy BJ, Watanabe K, et al. Massive Dirac fermions and Hofstadter butterfly in a van der Waals heterostructure. Science. 2013; 340: 1427-1430.
11. Dean C R, Wang L, Maher P, Forsythe C, Ghahari F, Gao Y, et al. Hofstadter's butterfly and the fractal quantum Hall effect in moire superlattices. Nature. 2013; 497: 598-602.

12. Schwierz F. graphene transistors. Nat Nanotechnol. 2010; 5: 487-497.

13. Nath P, Sanyal D, Jana D. Semi-metallic to semiconducting transition in graphene nanosheet with site specific co-doping of boron and nitrogen. Physica E. 2014; 56: 64-68.

14. Shinde PP, Kumar V. Direct band gap opening in graphene by BN doping: ab initio calculations. Phys Rev B. 2011; 84: 125401-125406.

15. Kuila T, Bose S, Mishra AK, Khanra P, Kim NH, Lee JH. Chemical functionalization of graphene and its applications. Prog Mater Sci. 2012; 57: 1061-1105.

16. Ni ZH, Xu T, Lu YH, Wang YY, Feng YP, Shen ZX. Uniaxial strain on graphene: Raman spectroscopy study and band-gap opening ACS Nano. 2002; 2: 2301-2305.

17. Nath P, Sanyal D, Jana D. Optical properties of transition metal atom adsorbed graphene: a density functional theoretical calculation. Phys E. 2015; 69: 306-315.

18. Chowdhury S, Das R, Nath P, Jana D, Sanyal D. Electronic and optical properties of boron- and nitrogen-functionalized graphene nanosheet. In: Thakur VK, Thakur MK, editors. Chemical functionalization of carbon nanomaterials: chemistry and applications. New York, NY: CRC Press. 2015; 42: 949-957.

19. Jana D, Nath P, Sanyal D, Ali N, Milne WI, et al. In: Alioflkhazraei M, editors. Modification of electronic properties of graphene by boron (B) and nitrogen (N) substitution. New York NY: CRC Press, Taylor & Francis. 2016; 231-246.

20. Kepler J. Weltharmonik II. Buch der Weltharmonik (R. Oldenbourg Verlag, Munchen-Berlin). 1939; 63.

21. Aleksey KI. Hypothetical planar and nanotubular crystalline structures with five interatomic bonds of Kepler nets type. AIP Adv. 2017; 7: 025202.

22. Balaban AT. Carbon and its nets. Comput Mat Appl. 1989; 17: 397-416.

23. Enyashin AN, Ivanovskii AL. Graphene allotropes. Phys Status Solidi B. 2011; 248: 1879-1883.

24. Baughman RH, Eckhardt H, Kertesz M. Structure-property predictions for new planar forms of carbon - layered phases containing sp2 and sp atoms. J Chem Phys. 1987; 87: 6687-6699.

25. Li Y, Xu L, Liu H, Li Y. Graphdiyne and graphyne: from theoretical predictions to practical construction. Chem Soc Rev. 2014; 43: 2572-2586.

26. Kehoe JM, Kiley JH, English JJ, Johnson CA, Petersen RC, Haley MM. Carbon Networks Based On Dehydrobenzoannulenes. 3. Synthesis of Graphyne Substructures. Org Lett. 2000: 2: 969-972.

27. Li G, Li Y, Liu H, Guo Y, Zhu D. Architecture of graphdiyne nanoscale films. Chem Commun. 2010; 46: 3256-3258.

28. Peng Q, Dearden AK, Crean J, Han L, Liu S, Wen X, et al. New materials graphyne, graphdiyne, graphone, and graphane: review of properties, synthesis, and application in nanotechnology. Nanotechnol Sci Appl. 2014; 7: 1-29.

29. Luo G, Qian X, Liu H, Qin R, Zhou J, Li L, et al. Quasiparticle energies and excitonic effects of the two-dimensional carbon allotrope graphdiyne: Theory and experiment. Phys Rev B. 2011; 84: 075439.

30. Zhu H, Balaban AT, Klein DJ, Zivkovic TP. Conjugated circuit computations on two dimensional carbon networks. J Chem Phys A. 1994; 101: 5281-5292.

31. Sadhukhan B, Nayak A, Mookerjee A. Effect of doping on the electronic properties of Graphene and T-graphene: A theoretical approach. Mesoscale Nanoscale Phy. 2017.

32. Liu Y, Wang G, Huang Q, Guo L, Chen X. Structural and Electronic Properties of T Graphene: A Two-Dimensional Carbon Allotrope with Tetrarings. Phys Rev Lett. 2012; 108: 225505.

33. Kim BG, Jo JY, Sim HS. Comment on "Structural and Electronic Properties of T Graphene: A Two-Dimensional Carbon Allotrope with Tetrarings" Phys Rev Lett. 2013; 110: 029601.

34. Kotakoski J, Krasheninnikov AV, Kaiser U, Meyer JC. From point defects in graphene to two-dimensional amorphous carbon. Phys Rev Lett. 2011; 106: 105505.

35. Ye XJ, Liu CS, Zhong W, Zeng Z, Du YW. Metalized T graphene: A reversible hydrogen storage material at room temperature. J Appl Phys. 2014; 116: 114304.

36. Liu CS, Jia R, Ye, Zeng Z. Non-hexagonal symmetry-induced functional T graphene for the detection of carbon monoxide. J Chem Phys. 2013; 034704.

37. Majidi R. Electronic properties of T graphene-like CBN sheets: a density functional theory study. Phys E. 2015; 74: 371-376.

38. Bandyopadhyay A, Pal P, Chowdhury S, Jana D. First principles Raman study of boron and nitrogen doped planar T-graphene clusters. Mater Res Express. 2015; 2: 095603.

39. Das R, Dhar N, Bandyopadhyay A, Jana D. Size dependent magnetic and optical properties in diamond shaped graphene quantum dots: A DFT study. J Phys Chem Solids. 2016; 99: 34-42.

40. Chowdhury S, Majumdar A, Jana D. Search for magnetism in transition metal atoms doped tetragonal graphene: A DFT approach. J Magn Mater. 2017; 441: 523-530.

41. Sheng XL, Cui HJ, Ye F, Yan QB, Zheng QR, Su G. Octagraphene as a versatile carbon atomic sheet for novel nanotubes, unconventional fullerenes, and hydrogen storage. J Appl Phys. 2012; 112: 074315.

42. Zhang Y, Lee J, Wang WL, Yao DX. Two-dimensional octagon-structure monolayer of nitrogen group elements and the related nano structures. Comput Mater Sci. 2015; 110: 109-114.

43. Wang XQ, Li HD, Wang JT. Structural stabilities and electronic properties of planar C_4 carbon sheet and nanoribbons. Phys Chem Chem Phys. 2012: 14: 11107-11111.

44. Bandyopadhyay A, Nandy A, Chakrabarti A, Jana D. Optical properties and magnetic flux-induced electronic band tuning of a T-graphene sheet and nanoribbon. Phys Chem Chem Phys. 2017; 19: 21584-21594.

45. Dai CJ, Yan XH, Xiao Y, Guo YD. Electronic and transport properties of T-graphene nanoribbon: Symmetry dependent multiple Dirac points, negative differential resistance and linear current-bias characteristics. Euro phys Lett. 2014; 107: 37004.

46. Chowdhury S, Bandyopadhyay A, Dhar N, Jana D .Optical and magnetic properties of free-standing silicene, germanene and T-graphene system. Phys Sci Rev. 2017; 2: 20170102.

47. Chowdhury S, Jana D. A theoretical review on electronic, magnetic and optical properties of silicene. Rep Prog Phys. 2016; 79: 126501.

48. Wang J, Deng S, Liu Z, Liu Z. The rare two-dimensional materials with Dirac cones. Natl sci rev. 2015; 16: 1-18.

49. Kong X, Liu Q, Zhang C, Peng Z, Chen Q. Elemental two-dimensional nanosheets beyond graphene. Chem Soc Rev. 2017; 46: 2127-2157.

50. Schwingenschlogl U, Zhu J, Morishita T. Elemental Two-Dimensional Materials beyond Graphene. Phys Sci Rev. 2017.

51. Ordejon P, Artacho E, Soler JM. Self-consistent order N density functional calculations for very large systems. Phys Rev B Condens Matter. 1996; 53: R10441-R10444.

52. Portal DS, Ordejon P, Artacho E, Soler JM. Density-functional method for very large systems with LCAO basis sets. Int J Quantum Chem. 1997; 65: 453-461.

53. Soler JM, Artacho E, Gale JD, Garca A, Junquera J, Ordejon P, et al. The SIESTA method for ab initio order-N materials simulation. J Phys Condens Matter. 2002; 14: 2745-2779.

54. Monkhorst HJ, Pack DJ. Special points for Brillouin-zone integrations. Phys Rev B Solid State. 1976; 13: 5188-5192.

55. Jana D, Sun CL, Chen LC, Chen H. Effect of chemical doping of boron and nitrogen on the electronic, optical, and electrochemical properties of carbon nanotubes. Prog Mater Sci. 2013; 58: 565-635.

56. Jana D, Chen LC, Chen CW, Chattopadhyay S, Chen KH. A First Principles Study of optical properties of B_xC_y single wall nanotubes. Carbon. 2007; 45: 1482-1491.

57. Jana D, Chakraborty A, Chen LC, Chen CW, Chen KH. First-principles calculations of the optical properties of CxNy single walled nanotubes. Nanotechnol. 2009; 20: 175701-175712.

58. Nath P, Chowdhury S, Sanyal D, Jana D. Ab-initio calculation of electronic and optical properties of nitrogen and boron doped graphene nanosheet. Carbon. 2014; 73: 275-282.

59. Rani P, Dubey GS, Jindal VK. DFT study of optical properties of pure and doped graphene. Physica E Low-dimensional Systems Nanostructures. 2014; 62: 28-35.

Cite this article

Bandyopadhyay A, Jana D (2017) A Detailed First Principles Investigation of Optical Properties of Monolayer T-Graphene Sheet and Nanoribbon. JSM Nanotechnol Nanomed 5(3): 1057.